Feasibility of electromagnetic methods for sub-basalt exploration

Jostein Herredsvela, Arnout Colpaert, Stig-Kyrre Foss, Anh Kiet Nguyen, and Ketil Hokstad, Statoil
Jan Petter Morten, Claudia Twarz, Stein Fanavoll, and Frida Mrope, EMGS

Summary

Seismic imaging can be challenging in basalt regions, and we consider how EM methods can be used to enhance understanding in exploration. For a synthetic basalt model, we consider the sensitivity and inversion of CSEM and MT data, and discuss the dependence on anisotropy and water depth. Our inversion results demonstrate how the combination of EM methods resolves the base basalt depth and sub-basalt structure.

Introduction

Basalts are extrusive volcanic rocks, associated with volcanic eruptions or rifting. Basalts are encountered worldwide, especially on the continental seafloor, but can also be found in both small and large igneous provinces onshore.

The form, structure and texture of basalt are strongly dependent on the environment in which it erupted and the chemical composition of the lava. Subaerial basalts are characterized by a very complex stacking of individual lava flows, with rugose and altered clay-rich zones near top and bottom of the individual flow and a clean non-altered core in the middle. The thickness of the flow varies from a meter up to tens of meters. The core and the altered top reveal highly variable material properties (e.g. density, electrical resistivity, porosity). Subaqueous basalts are often present below subaerial basalts in offshore basalt deltas, and consist of both pillow lavas and hyaloclastites. Their stacking is often less cyclic, but alteration of the glassy material and presence of tuff introduces also in these basalts a large variation in material properties. Seismic scale geometries and rugose surfaces both within and at the base of the stacked subaqueous volcanic sequences are commonly observed. Sediment packages can be embedded between different lava flows.

The most commonly used method for marine exploration is seismic. The above mentioned properties of a volcanic sequence imply that there are large impedance contrasts within the basalt package. This causes difficulties for exploration of sub-basalt regions, and it is often extremely difficult to obtain reliable seismic images of sub-basalt geology. In addition to water-layer and peg-leg multiples, the layered flow basalts cause a huge amount of very short-period intra-layer multiples, and the subaqueous part scatters the seismic energy in all directions. The net effect is that most of the energy is scattered away from the basalt body, and that only the very lowest frequencies remain in the signal. Thus sub-basalt reflections are extremely weak, complicating processing and imaging. In summary, the base basalt and sub-basalt structure is often not well resolved in seismic, and complementary methods to aid sub-basalt exploration are required.

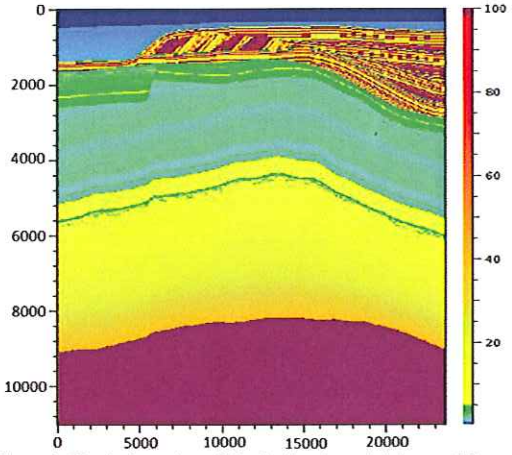

Figure 1: Vertical section of the the basalt resistivity model studied in this paper. This model has detailed internal structure in the basalt. We also study an effective model with a homogeneous basalt layer, but otherwise identical.

Non-seismic methods for sub-basalt exploration, such as gravity and electromagnetic (EM) methods are believed to be able to circumvent some of the obstacles faced by the seismic method. This is mainly because these methods rely on measurements with resolution less than the typical layer thicknesses and scatterer dimensions in the basalt. In this way, EM methods will probe effective basalt properties on a larger scale than seismic. Due to the complementary nature of the data, it is expected that the combination of EM methods with seismic can greatly aid understanding of basalt regions. For a recent application to land data, see Colombo et al. (2012).

In this paper we will consider how marine controlled source electromagnetic (CSEM) methods as well as magnetotellurics (MT) can be used to resolve a basaltic layer and sub-basalt structure in a synthetic model (Figure 1). We will consider the data sensitivity dependence on anisotropy, basalt thickness, and show how the airwave encountered in shallow water CSEM contributes to the sensitivity. We then discuss how the results could be useful in exploration, emphasizing resolution and depth penetration.

DOI http://dx.doi.org/10.1190/segam2012-0590.1

Synthetic basalt model

In this paper, we will study the 3D synthetic model shown with a vertical section in Figure 1. The water depth is 300-350 m. The model consists of a basaltic delta of variable thickness, from 200 m to 2 km, above conductive sediments. The basalt is mostly located close to the seafloor, at a burial depth about 100-200 m. The underlying sediment package has resistivity 1.5-10 Ωm, and is about 7 km thick. Under the sediments, the model has a basement at 1000 Ωm. The basalt shown in Figure 1 has a lot of internal structure which is based on observations from well logs and seismic. The layers comprising the basalt have variable resistivity between 5 and 10^6 Ωm, and the layers have variable dip angle up to 40 degrees. Depending on the deposition history, basalt may have curvature in the strike direction. There is a gentle bend of the layers in the direction transverse to the plane shown in Figure 1, but modeling showed that the data could be approximated well by assuming invariance in the transverse direction.

The intra-basalt detail level in the model of Figure 1 cannot be recovered from electromagnetic surface data, which will be limited to low frequencies due to dissipation. Rather, the data can resolve effective properties on length scales corresponding to those of signal propagation. To understand the nature of such effective models that could be produced by inversion, we have compared the data from the model in Figure 1 to the data obtained from models obtained using various upscaling approaches. Where data are affected by layers with large dip angle, our results (not shown) demonstrated significant deviation between the original model data and those obtained from upscaled models that were transverse isotropic with a vertical axis of symmetry (TIV). This indicates that a tilted transverse isotropic (TTI) model representation should be adopted to avoid artifacts when inverting the data from the original model. However, in the following study we will consider a simplified case where the basalt layer is represented as a homogeneous TIV medium.

In the following, we consider effective basalt models and replace the internal structure in the basalt shown in Figure 1 by a homogeneous layer. The geometry of the basalt layer and all other layers are kept as in Figure 1. We consider that the basalt layer has 55 Ωm vertical resistivity, and 8 Ωm horizontal resistivity. The effective value for the horizontal resistivity represents a lower estimate, in order to study the performance of EM imaging for a very difficult case with little horizontal resistivity contrast to the background. The resistivity of the layers below the basalt is typically 6 Ωm. The large basalt anisotropy could arise due to alternating conductive and resistive layers in the vertical direction. However, in situations where such regular intra-basalt structure is not present or is random on the length scales of the signal propagation, the effect of the intra-basalt layering averages out for the effective medium and the basalt could appear as isotropic. Results reported by Abubakar et al. (2011) considering inversion of real data from the More basin in Norway demonstrated CSEM imaging of a basalt layer in an isotropic model. On the other hand, an onshore MT study by Pandey et al. (2008) indicates a highly anisotropic flow basalt section within the Deccan traps, India. Therefore, we will study both the case of anisotropic and isotropic basalt in the following. We will consider a 2D survey layout, with 43 receivers at 500 m spacing. For these receivers, we will discuss the sensitivity and inversion of inline and broadside CSEM data, as well as MT data. Note that the broadside CSEM data considered here corresponds to the measurements obtained from azimuth receivers in 3D CSEM acquisition.

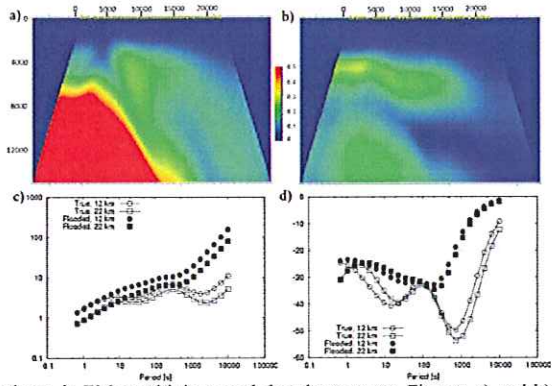

Figure 2: EM sensitivity to sub-basalt structure. Figures a) and b) show inline and broadside CSEM normalized data difference at 0.39 Hz between true model and basalt-flooded model, $|E_{True}-E_{Flood}|/|E_{True}|$, common mid-point (CMP) sorted. The color scale ranges from 0.0 to 0.5. Bottom row shows the transverse magnetic MT apparent resistivity [Ωm] c) and phase [degrees] d) data for the true and flooded models for receivers located at positions 12 km and 22 km in Figure 1.

To quantify the sensitivity to sub-basalt structure, we will compare to data from a flooded model, where the basalt layer is continued downwards indefinitely. We will first consider the model where basalt is anisotropic. Figure 2 shows the simulation results for inline and broadside CSEM data, as well as MT responses. Where the basalt layer is thin, all three measurements will have significant sensitivity to sub-basalt structure. However, the sensitivity diminishes when the basalt thickness grows above 1 km, and we when consider MT frequencies above 0.3 Hz. Lower frequencies that penetrate deeply will retain sensitivity for thick basalt for MT as well as broadside CSEM, but can only give imprecise information about the base basalt depth due to the long wavelength. There is a considerable vertical resistivity contrast between basalt and background in the model to which inline CSEM data will be sensitive. The sensitivity will still be low, however, due to the so-called guided wave which will dominate the

DOI http://dx.doi.org/10.1190/segam2012-0590.1

response and has limited sensitivity towards basalt thickness as discussed in Morten et al. (2011).

Figure 3 shows the same sensitivity plots as in Figure 2, but now we have considered an isotropic model where both resistivity components equal the vertical resistivity of the model considered previously. In the isotropic model, all the measurements considered have good sensitivity to sub-basalt structure. We therefore expect reliable imaging results even when taking into account the finite measurement accuracy of real data.

CSEM sensitivity dependence on water depth

Measurements that involve predominantly horizontally polarized electromagnetic fields will have stronger sensitivity towards conductive, horizontal layers than measurements mainly controlled by vertically polarized fields. This is analogous to the concepts of parallel and series coupling in circuit theory, where the surface measurements using horizontally polarized fields correspond to a parallel coupling of the layers. In the context of imaging conductive sedimentary layers below resistive basalt, we can therefore expect a large sensitivity difference between inline CSEM measurements acquired in deep and shallow water. This is because of the airwave (Løseth, 2007; Andreis and MacGregor, 2008; Løseth, 2011), which is a horizontally polarized field generated at the air-water interface, similar to the source for MT responses. In deep water, this signal is attenuated during propagation in the water column, but in shallow water it can constitute a large contribution to the response.

Sub-basalt imaging in an ultra-deep water case was discussed in Morten et al. (2011), and it was found that sufficient sensitivity could only be restored from CSEM data in the broadside configuration obtained in 3D surveys. For the present case of water depth 300-350 m, we saw in Figure 3 that in the isotropic basalt case the inline data sensitivity for the thickest basalt (2 km) was as large as that for thin basalt (0.2 km). This situation is qualitatively different from the ultra-deep water case. The practical implication of this behavior is that conventional inline CSEM data will be efficient for determining sub-basalt structure in shallow water when there is a horizontal conductivity contrast to the background and the model can be approximated as 2D. An advantage of these measurements over MT is that the frequency spectrum of the source can be controlled. We may therefore design the survey such that the depth resolution to the base of basalt can be optimized.

Inversion results

We will now consider inversion results where we have used the effective model with homogeneous basalt to generate

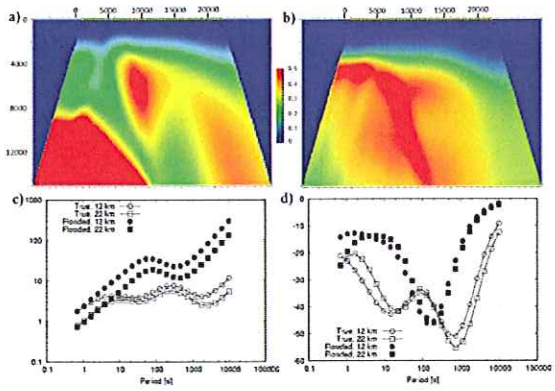

Figure 3: EM sensitivity to sub-basalt structure, same plots as in Figure 2 but considering isotropic basalt (55 Ωm) model.

the input data. We have used basalt flooded models with the correct top basalt interface as initial models for the CSEM inversions. The CSEM inversions were carried out using data from frequencies 0.11, 0.39, and 0.88 Hz, and the MT inversions considered 23 frequencies logarithmically distributed in the interval 10^{-4} to 1.43 Hz. The CSEM data maximum offset was restricted such that only data with signal strength expected to be significant over noise in a real acquisition are included. No noise was added to the data. Since our modeling analysis indicated that the model could be treated as 2D, we used 2.5D and 2D inversion software for the CSEM and MT inversions respectively. The CSEM inversion algorithm was described by Hansen and Mittet (2009), and the MT data was processed with an Occam inversion (Constable et al., 1987). The MT inversion was performed with an isotropic code considering only the horizontal resistivity.

Figure 4 shows inversion results for the anisotropic basalt model for CSEM and MT data. Both inversions have recovered the basalt layer, but with variable resolution of the thin and thick basalt regions respectively. The CSEM inversion was able to recover the base basalt interface to accuracy 100 to 300 m up to a basalt thickness of about 1500 m. In particular, the thin basalt regions are well defined. The MT inversion is not sensitive to the thinnest part of the basalt, but was better able to recover the base basalt depth for the thickest part (2 km). Furthermore, the low frequencies included in the MT dataset allowed imaging of the basement structure.

Figure 5 shows the CSEM inversion result for the isotropic case with sensitivities shown in Figure 3. As expected, the large sensitivity towards sub-basalt structure is giving a good inversion result and even the thickest basalt region is imaged with 200-300 m precision for the base basalt interface when using the inline data. The regularization approach used in the CSEM inversion resulted in sharp,

DOI http://dx.doi.org/10.1190/segam2012-0590.1

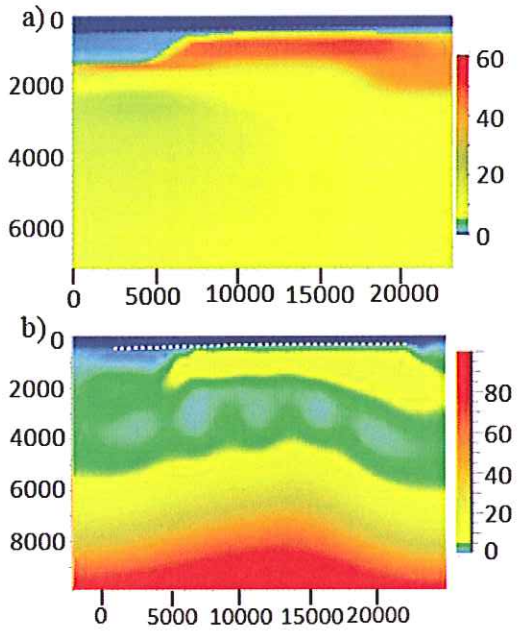

Figure 4: Inversion results for the model with basalt resistivity 55/8 Ωm for vertical/horizontal components. Figure a) shows the vertical resistivity recovered by CSEM data. Figure b) shows the resistivity recovered from isotropic MT inversion considering the horizontal resistivity component.

horizontal interfaces where the information in the input data was insufficient to constrain the model geometry precisely. Broadside data gives a model exhibiting more structure as could be expected from Figure 3 which indicates larger sensitivity at more offsets. MT inversion on the same isotropic model gives a result qualitatively similar to the one shown in Figure 4, but with larger resistivity in the basalt.

Value of EM imaging results in exploration

We have demonstrated how EM methods can be used to image the various features of a basalt model with geometries as shown in Figure 1. Specifically for this case of shallow water, inline CSEM data gives good sensitivity towards the base basalt interface which is mapped with a precision of 200-300 m even up to basalt thickness 2 km in the isotropic case. The basalt and underlying sediments are imaged with approximately correct resistivity values. The MT data is particularly useful for the thicker basalt sections, and additionally images the deeper basement and some details of the sediment package.

We believe that such results could be of significant value in an exploration case where seismic imaging performs poorly. The resistivity information in the EM results could allow for identification of basalt layers, and the imaged

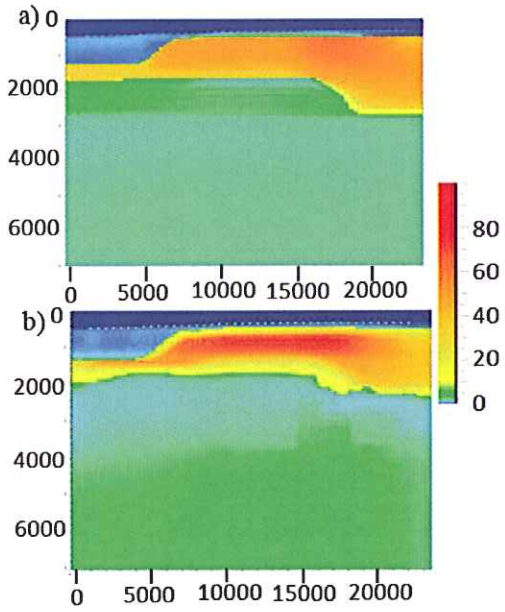

Figure 5: CSEM inversion results for isotropic model with 55 Ωm in the basalt using a) only the inline data or b) only broadside data.

geometries might make the interpreter capable of identifying basalt reflectors when comparing to seismic imaging results. Moreover, the precision of the recovered basalt geometry could be valuable input for velocity model building, and allow for improved seismic imaging. Finally, we would like to point out that the results in this paper are inherently model-dependent, and full generalization cannot be expected for all the behaviors observed

Conclusions

We have considered basalt imaging using EM methods for a synthetic basalt model. We considered the effect of regular internal structure in the basalt, and discuss anisotropy. The sensitivity in different scenarios is studied, and we find that in shallow water the airwave in CSEM data enhances sensitivity to sub-basalt structure. The inversion results indicate that basalt geometry and resistivity can be recovered from the EM data, as well as the sub-basalt structures.

Acknowledgments

We thank Statoil and EMGS for permission to show these results. We acknowledge Mark Rhodes, Max Åmark, and Roald Lindgren of Statoil, and David Kessler of SeismicCity for contributing to the creation of the synthetic basalt model. We also acknowledge Statoil's Sub-basalt task force for valuable discussions and input.

DOI http://dx.doi.org/10.1190/segam2012-0590.1

http://dx.doi.org/10.1190/segam2012-0590.1

EDITED REFERENCES

Note: This reference list is a copy-edited version of the reference list submitted by the author. Reference lists for the 2012 SEG Technical Program Expanded Abstracts have been copy edited so that references provided with the online metadata for each paper will achieve a high degree of linking to cited sources that appear on the Web.

REFERENCES

Abubakar, A., M. Li, G. Pan, J. Liu, and T. M. Habashy, 2011, Joint MT and CSEM data inversion using a multiplicative cost function approach: Geophysics, **76**, no. 3, 203–214.

Andréis, D., and L. M. MacGregor, 2008, Controlled-source electromagnetic sounding in shallow water: Principles and applications: Geophysics, **73**, no. 1, 21–32.

Colombo, D., T. Keho, and G. McNeice, 2012, Integrated seismic-electromagnetic workflow for sub-basalt exploration in northwest Saudi Arabia: The Leading Edge, **31**, 42–52.

Constable, S. C., R. L. Parker, and C. G. Constable, 1987, Occam's inversion — A practical algorithm for generating smooth models from electromagnetic sounding data: Geophysics, **52**, 289–300.

Løseth, L. O., 2011, Insight into the marine controlled-source electromagnetic signal propagation: Geophysical Prospecting, **59**, 145160.

Løseth, L. O., 2007, Modelling of controlled source electromagnetic data: Ph.D. thesis, Norwegian University of Science and Technology.

Morten, J. P., S. Fanavoll, F. M. Mrope, and A.K. Nguyen, 2011, Sub-basalt imaging using broadside CSEM: 73rd Conference & Exhibition, EAGE.

Pandey, D. K., L. M. MacGregor, M. C. Sinha, and S. C. Singh, 2008, Feasibility of using magnetotelluric for sub-basalt imaging at Kachchh, India: Applied Geophysics, 5, 74–82.

Rymann Hansen, K. and R. Mittet, 2009, Incorporating seismic horizons in inversion of CSEM data, 79th Annual International Meeting, SEG, Expanded Abstracts, 694–698.

DOI http://dx.doi.org/10.1190/segam2012-0590.1